Computational Study of the Particles Interaction Distance under the Influence of Steady Magnetic Field

N. K. Lampropoulos[1], E. G. Karvelas [1,2] and I. E. Sarris[1]

[1] *Department of Energy Technology, Technological & Educational Institute of Athens, Ag. Spyridona 17, 12210 Athens, Greece.*

[2] *Department of Civil Engineering, University of Thessaly, Volos, Greece.*

Abstract

A computational method for the estimation of the particles' maximum interaction distance, when these are under the influence of a steady magnetic field, is presented. The computational model was developed for the simulation of the particles and the forces that are exerted on them. The chains of particles are formed under the influence of these forces. Also, the mean value of cogglomeration is estimated with simulations, which have different number of particles under a steady concentration and a uniform magnetic field.

Keywords Interaction distance, Magnetic driving, Aggregations

1 Introduction

For the treatment of serious diseases, drug is inserted into the human body through a blood vessel and through the blood circulation reaches the infected area. As a result of the above mentioned injection, the drug circulates all over the human body and causes damages in areas that are not infected. In order to overcome this difficulty, we attach drug to particles and drive them to the infected area. For the particles' guidance to the targeted area, a Magnetic Resonance Imaging (MRI) device is needed. This method was presented for the first time in the 1970's [1, 2]. It minimizes the side effects, as the drug is driven only to the infected area. The above mentioned method is applied with even better results on small blood vessels with low blood flow rates [3]. Other factors that affect the efficiency of the proposed method is the size, the material of the particles and the magnetic intensity. The smaller a particle is, the smaller the magnetic response will be. As a result, the magnetic driving to the infected area is non-feasible [4,5]. To overcome this problem, magnetic particles are used in order to form cogglomerates [6]. It is proven that the total magnetic moment of cogglomerates is higher than this of the isolated particles, and therefore, clusters are more magnetically responsive [7]. Consequently, the magnetic driving is feasible. When the aggregates reach the targeted area, break into isolated particles. This is feasible with the usage of superparamagnetic particles, which lose their magnetism when there is no magnetic field [6].

It is verified that the computational methods can simulate with accuracy or with a small discrepancy the experimental data [8]. Interaction distance of par-

ticles plays an important role in the accuracy of the results, when these are compared with the experimental data. The minimum interaction distance is chosen, in order to export accurate results in minimum time, because the magnetic moments that are exerted on a particle are calculated from particles that are located inside the minimum interaction distance. The aim of this study is to define the minimum particle's interaction distance under a constant magnetic field.

The forces acting on a particle are described in section 2 and the results in section 3. Finally, discussion is presented in section 4.

2 Numerical Model

For the propulsion model of the particles, four major forces are considered, i.e. the magnetic force from MRIs Main Magnet static field, as well as the Magnetic field gradient force from the special Propulsion Gradient Coils. The static field caters for the aggregation of nanoparticles, while the magnetic gradient navigates the agglomerations. Moreover, the contact forces among the aggregated nanoparticles and the wall is used. The Stokes drag force for each particle is considered, while only spherical particles are used in the calculation process. Finally, gravitational forces due to gravity and the force due to buoyancy are added.

The motion of particles is given by the Newton equations.

$$m_i \frac{\partial \boldsymbol{u}_i}{\partial t} = \boldsymbol{F}_{mag\_i} + \boldsymbol{F}_{nc\_i} + \boldsymbol{F}_{tc\_i} + \boldsymbol{F}_{hydro\_i} + \boldsymbol{F}_{boy\_i} + \boldsymbol{W}_i \tag{1}$$

$$\boldsymbol{I}_i \frac{\partial \omega_i}{\partial t} = \boldsymbol{M}_{drag\_i} + \boldsymbol{M}_{con\_i} + \boldsymbol{T}_{mag\_i} \tag{2}$$

where the index i stands for the particle i. All quantities indicated in (1) and (2) are presented in Table 1 and depicted in Figure 1. The bold variables represent vector quantities. The numerical model for the forces is given in [8].

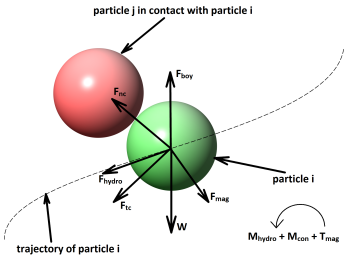

Fig. 1 Forces and moments of a particle.

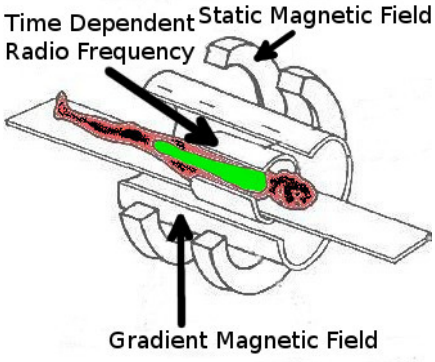

Fig. 2 Domain of particle close magnetic field inside the MRI bore.

2.1 Magnetic Field in the MRI bore

The magnetic field $\boldsymbol{B}$ in the MRI bore is given by

$$\boldsymbol{B} = \boldsymbol{B}_0 + \tilde{\boldsymbol{G}} + \boldsymbol{B}_1 \tag{3}$$

and is depicted in Figure 2. $\boldsymbol{B}_0$ is the MRI superconducting magnet field that is constant and uniform, $\tilde{\boldsymbol{G}}$ is the gradient field and $\boldsymbol{B}_1$ is the time dependent radio frequency field [9]. The steady magnetic field $\boldsymbol{B}_0$ is used for the cogglomeration forming and the gradient magnetic field $\tilde{\boldsymbol{G}}$ for the navigation of the cogglomerates into the desired area.

2.2 Particle's Interaction Distance

The magnetic interaction force, F, in the parallel direction between two spheres is inversely proportional to the fourth power of the separation distance [10, 11]:

$$\boldsymbol{F} \propto \frac{M_i M_j}{(h + a_i + a_j)^4} \tag{4}$$

where, M_i and M_j are the magnetic moments of the center of each sphere and h is the nearest distance between the surfaces of two spheres with radii a_i and a_j.

Although, a weak interaction is being observed for particles that are more than five radii apart, as time goes by, the interaction force is getting stronger, because the particles are getting faster closer to each other [8].

This study is trying to define the minimum interaction distance D_i of the particle, as is depicted in Figure **??**, in which the mean length of aggregations remains stable. To estimate the minimum particle's interaction distance, five series of simulations were performed with 100, 200, 300, 400, 500 particles, respectively. For each series, fifteen simulations have been performed. Each time, the particle's interaction distance varied from 5 to 20 radius.

Table 1 Forces and moments

Simulation Quantities	
Quantity	Description
$\boldsymbol{v}_i$	Velocity
$\boldsymbol{\omega}_i$	Rotational Velocity
t	Time
$\boldsymbol{I}_i$	Mass moment of inertia matrix
m_i	Mass
$\boldsymbol{F}_{mag\_i}$	Total applied magnetic force
$\boldsymbol{F}_{nc\_i}$	Normal contact force
$\boldsymbol{F}_{tc\_i}$	Tangential contact force
$\boldsymbol{F}_{boy\_i}$	Buoyancy force
$\boldsymbol{W}_i$	Weight force
$\boldsymbol{F}_{drag\_i}$	Drag force
$\boldsymbol{M}_{drag\_i}$	Drag moments
$\boldsymbol{M}_{con\_i}$	Contact moments
$\boldsymbol{T}_{mag\_i}$	Torque due to the magnetic field

3 Numerical Method

The OpenFoam platform was used in order to calculate the flow field and the uncoupled equations of particles' motion [12]. The simulation process reads as follows: Firstly, the fluid flow is found using the pressure correction method. Upon finding the flow field (pressure, velocity) the motion of particles is evaluated by the Lagrangian method by solving Eq. (1) and (2) along the trajectory of each particle. The equations are solved in time using the Euler time marching method. The stability of the algorithm is guaranteed with a time step of $10^{-6}s$.

Table 2 Simulation parameters

Flow domain and computational grid of Case 1 (3D)						
No	Concentr. (mg/ml)	Particles	Volume (m^3)	Dimension in x-dir (m)	Dimension in y-dir (m)	Dimension in z-dir (m)
1	1.125	100	7.303×10^{-11}	4.18×10^{-4}	4.18×10^{-4}	4.18×10^{-4}
2	1.125	200	1.381×10^{-10}	5.17×10^{-4}	5.17×10^{-4}	5.17×10^{-4}
3	1.125	300	2.018×10^{-10}	5.94×10^{-4}	5.83×10^{-4}	5.83×10^{-4}
4	1.125	400	2.686×10^{-10}	6.6×10^{-3}	6.38×10^{-3}	6.38×10^{-5}
5	1.125	500	3.489×10^{-10}	7.04×10^{-4}	7.04×10^{-4}	7.04×10^{-4}

The spacing of the computational grid is equal to $2 * diameter$ of the particles that were simulated. The summary of the domain parameters for the simulated cases is tabulated in Table 2.

4 Results

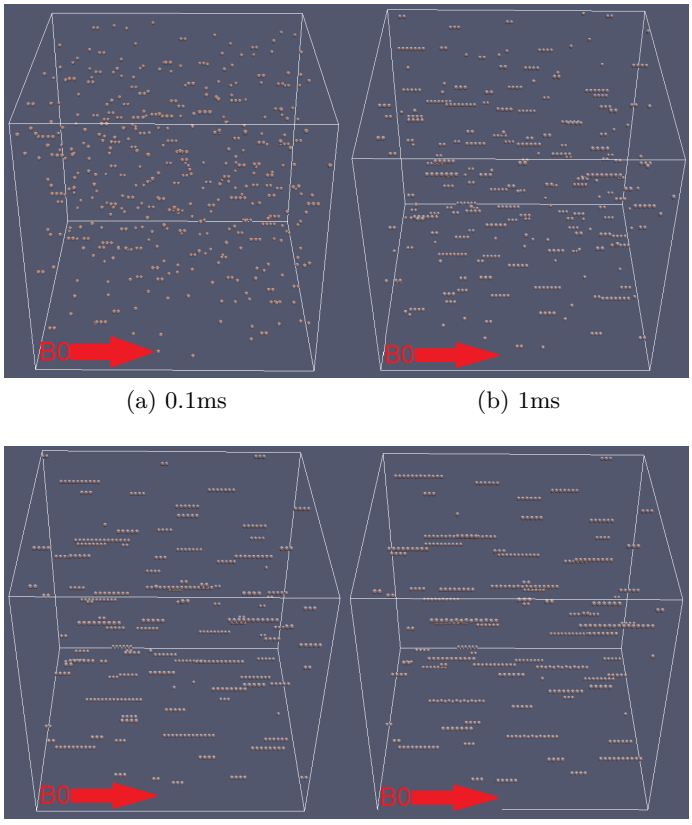

(a) 0.1ms (b) 1ms

(c) 3ms (d) 5ms

Fig. 3 Snapshots of aggregation process of 500 particles under a uniform magnetic field of $B_0 = 0.4T$.

Simulations with 100, 200, 300, 400, 500 particles were performed. For each number of particles, fifteen simulations were tested. Each time the particle's interaction distance varied from 5 to 20 radius with an increment of 1. The concentration and the magnetic field of the domain were 1.125 kg/m^3 and $0.4T$, respectively. The diameter of each particle was 11 um and the relative magnetic permeability (μ_r) of the Fe_3O_4 particles was 12.3. The Young modulus (Y) and the Poisson ratio (ν) of the material was 10^9 $m^{-2}Pa$ and 0.5, respectively. The tangential stiffness (γ) was 10 Nsm^{-1} and the coefficient of friction (μ) was 0.5 . The density of the fluidic environment (ρ_f) and particle (ρ_p) was 1000 and 1087 kg/m^3.

From Figure 4 is depicted that the mean length of the chains remains steady,

when the particle's interaction distance is more than 11 radius. The mean length and std deviation of aggregations are steady above 11 radii. On the other hand, when the particle's interaction distance is between 5 and 10 radii, the results show discrepancies from the experimental data. These discrepancies appeared due to truncation error, which is minimized when the particle's interaction distance is more than 11 radii. Apparently, the forces that are exerted on each particle are eliminated more than 11 radii when a magnetic field is applied. The computational platform does not estimate all the forces that are exerted on the particle from each neighbour, due to the existence of a certain interaction distance each time.

For the simulations of 200 to 500 particles, the mean length of aggregations that is estimated from the computational platform is in a good agreement with the experimental data, as is depicted in Figure 5. The simulations that were performed with 100 particles show a small discrepancy from the experimental data. This difference occurs due to the small numbers of particles that were used in the simulation, in comparison with the measurements that were conducted using a number of particles in the order of 10^6 .

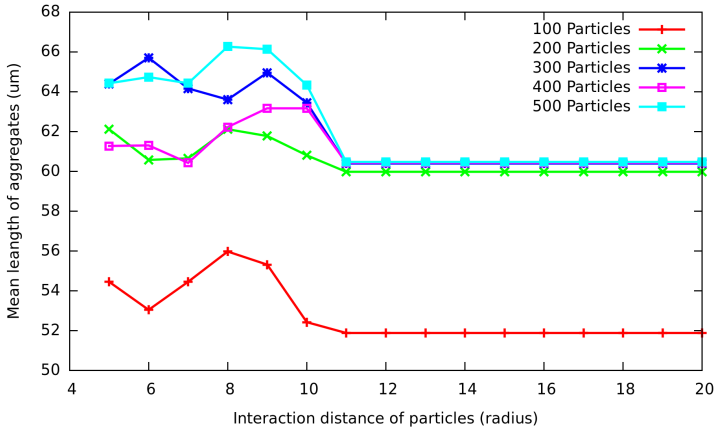

Fig. 4 Mean length of aggregations with different particle's interaction distance.

5 Discussion

After all the above mentioned simulations, it is observed that under the influence of a steady magnetic field of 0.4 T and concentration of 1.125 kg/m^3 the results are steady, when the particles interaction distance is above 11 diameters, as is depicted in Figure 4. In Figure 5, is observed that the computational platform estimates accurately the experimental data [6]. Although, in the simulations of 100 particles the computational platform shows discrepancies with the experimental data, in these with more particles the proposed method is in agreement

with the experimental data. The small number of particles is the cause of these discrepancies.

In Figure 3, we present some snapshots of the aggregation process. In time of $0.1ms$, the particles are isolated, as they have not form chains. From $1ms$ to $3ms$, chains are observed, but some particles are still isolated. They have, thus, the tendency to form aggregations either with other particles that are isolated or with the chains that are already formed. In time of $5ms$, the aggregation process has ended. As a result, the chains are the longest possible under the current magnetic field. Small number of particles is still isolated and they will not form aggregations as time goes by, because there is no force exerted on them.

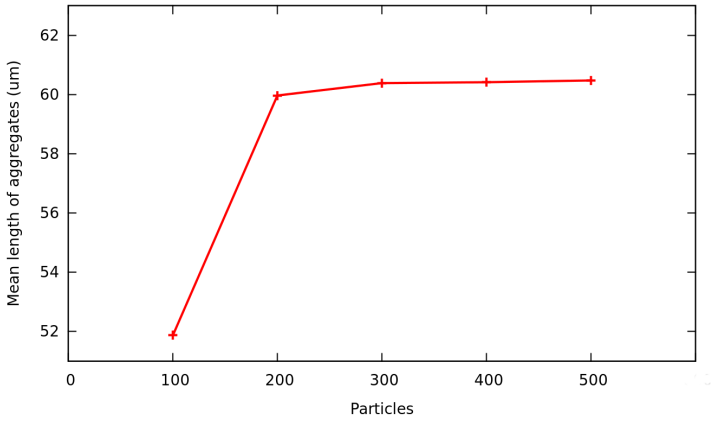

Fig. 5 Mean length of aggregations with different number of particles.

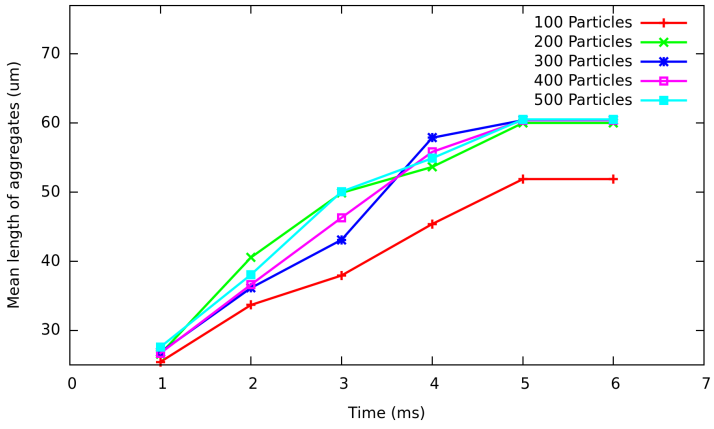

Fig. 6 Mean length of aggregations in each ms

In Figure 6, the aggregation process is presented in accordance with time. The

mean length of the aggregation is estimated for each ms of the process till its completion. The aggregation process is not linear, because the particles react with each other. As a result, the size of the chains is constantly changing. For tests of 100 particles, the aggregation process shows discrepancies with the other simulations, due to the small number of particles that has been simulated.

Factors, such as size, the material of the particles and the magnetic intensity of the field are important for the interaction distance. Higher intensity of the magnetic field creates stronger forces between particles. As a result, the particles interact in greater distances. Therefore, the mean length of aggregates tends to be larger. Bigger particles with the same magnetic intensity become into stronger magnets, due to bigger magnetic volume. As a result, smaller particles are attracted by bigger ones. The material of the particles plays an important role in the particles' interaction distance. Particles with high material magnetic susceptibility attract particles that are located in greater distances than those which have low. As a result of all the above, the interaction distance becomes greater.

6 Conclusion

In this work, a parametric study for the particles' interaction distance is presented. After the simulations, it was observed that there is no interaction between the particles, which have a distance above 11 diameters. The computational method simulated the experimental results with a minimal discrepancy.

Acknowledgments

The work is funded by the NANOTHER program (Magnetic Nanoparticles for targeted MRI Therapy) through the Operational Program COOPERATION 2011 of GSRT, Greece. Discussions with Dr Klinakis from BRFAA, Greece, Prof. Zergioti from NTUA, Greece and the people from Future Intelligence Ltd. are also acknowledged.

References

[1] A. Senyei, K. Widder, and C. Czerlinski, (1978), "Magnetic guidance of drug carrying microspheres," *Appl. phys.*, Vol. 49, pp. 3578–3583.

[2] K. Widder, A. Senyei, and G. Scarpelli, (1978), "Magnetic microspheres : a model system of site specific drug delivery in vivo." *Proc. Soc. Exp. Biol. Med.*, Vol. 158, pp. 141–146.

[3] B. Yellen, Z. Forbes, and D. Halverson, (2005), "Targeted drug delivery to magnetic implants for therapeutic applications," *Magn. Magn. Mater*, Vol. 293, pp. 647–54.

[4] Q. Pankhurst, J. Connolly, S. Jones, and J. Dobson, (2003), "Applications of magnetic nanoparticles in biomedicine," *Physiscs D:Applied Physics*, Vol. 36, pp. 166–181.

[5] O. Petracic, (2010), "Superparamagnetic nanoparticle ensembles," *Superlattices and Microstructures*, Vol. 47, p. 569.

[6] J.-B. Mathieu and S. Mantel, (2009), "Aggregation of magnetic microparticles in the context of targeted therapies actuated by a magnetic resonance imaging system," *J. Appl. Phys.*, Vol. 106, p. 044904.

[7] P. Babinec, A. Krafcik, M. Babincova, and J. Rosenecker, (2010), "Dynamics of magnetic particles in cylindrical halbach array: implicationsfor magnetic cell separation and drug targeting," *Med. Biol. Eng. Comput.*, Vol. 48, pp. 745–753.

[8] N. K. Lampropoulos, E. G. Karvelas, and I. E. Sarris, (2014), "Computational modeling of an MRI guided drug delivery system based on magnetic nanoparticle aggregations for the navigation of paramagnetic nanocapsules", under review.

[9] C. L. Epstein and F. W. Wehrli. (2005), "Magnetic resonance imaging," *Elsevier Encyclopedia on Mathematical Physics*, [Online]. Available: http://www.math.upenn.edu.

[10] T. Fujita and M. Mamiya, (1987), "Interaction forces between nonmagnetic particels in the magnetized magnetic fluid," *J. of Magnetism and Magnetic Materials*, Vol. 65, pp. 207–210.

[11] A. Mehdizadeh, R. Mei, J. F. Klausner, and N. Rahmatian, (2010), "Interaction forces between soft magnetic particles in uniform and non-uniform magnetic fields," *Acta Mechanica Sin.*, Vol. 26, pp. 921–929.

[12] H. G. Weller, G. Tabor, H. Jasak, and C. Fureby, (1998) "A tensorial approach to computational continuum mechanics using object-oriented techniques, *Computers in Physics*," Vol. 12, No. 6, pp. 620–631.

Corresponding author
E. G. Karvelas can be contacted at: karvelas@uth.gr